Extinction of a Stagnation-Point Diffusion Flame at Reduced Gravity

David W. Foutch* and James S. T'ien†
Case Western Reserve University, Cleveland, Ohio

The extinction limits of a diffusion flame in the stagnation-point boundary layer of a solid fuel in mixed-, natural-, and forced-convective flows are determined numerically. The flow is characterized by a mixed-convection stretch rate and a densimetric Froude number. The results depend primarily on stretch rate and only slightly on Froude number. The computed results show that in addition to the familiar blowoff limit, which occurs at large stretch rate, an extinction limit due to radiative heat loss from the fuel surface is found at very low stretch rate. These two extinction boundaries merge to define a fundamental low oxygen limit. The difference of this oxygen limit for forced and buoyancy-driven flows is found to be slight.

Introduction

THE dependence of diffusion flame extinction characteristics on the gravitational level has long been of scientific interest.[1-3] With intensified efforts directed toward manned space missions, an important fire-safety question arises: Are materials more or less flammable at reduced gravity than at one gravity? Although one may wish for a simple yes-or-no answer, the reality is more complex. In reduced gravity, although buoyancy-induced convection is diminished, it may not vanish completely. The effect of a low-speed flow induced by these low gravity levels on material flammability has not been investigated in the past. Furthermore, in many practical situations, such as the living quarters of a spacecraft, a slow forced-convective flow exists because of the need for ventilation. Thus, practical fire safety cannot be assured without an understanding of flame behavior in the presence of low-speed mixed convection.

In the limit of zero buoyancy-induced flow, the effect of a slow, forced-convective flow on the extinction limit of a solid fuel has recently been analyzed by T'ien.[4] It was found that at a given oxygen concentration, a flame can exist for a range of forced flow velocities. At very high speed, the familiar blowoff extinction limit was found. At very low speeds, another extinction limit was found when the effect of radiation from the solid surface was included. Because of this radiative loss, a flame could not exist at any velocity below a certain oxygen concentration. The possibility of radiative extinction has also been discussed by Bonne[5] and Sibulkin et al.[6]

At normal gravity, the speed of the gravity-induced flow would be great enough to prevent this radiative extinction branch from being observed for many fuels and geometries. T'ien's work assumed zero gravity. Even on a spacecraft, however, true zero gravity does not exist. Motor firings and crew movement can cause accelerations. For a flame in a low-speed forced flow, even a low gravity level cannot be neglected. So the behavior of a flame in a low-speed mixed-convection flow is of interest.

This work extends the analysis of T'ien to include mixed convection. The extinction limits of a flame at the stagnation point of a solid fuel in a mixed convective flow are investigated. The stagnation-point diffusion flame has been used to investigate many aspects of combustion science because it is particularly easy to analyze.[7,11] The mixed-convection flow at the stagnation point is characterized by a densimetric Froude number and by a mixed-convection velocity gradient similar to the one proposed by Fernandez-Pello and Law.[8] This work has two foci: 1) the effect of surface radiation on the extinction limits and 2) the effect of the type of convection—forced, natural, or mixed—on the extinction limits.

Model Formulation

The model used here is a modification of the one used by T'ien,[4] which in turn is based on Ref. 9. The physical situation being modeled is that of a flame in the stagnation region of a cylinder or sphere of solid fuel.

The assumptions are:

1) The forced flow is parallel to, and in a direction opposite to, the gravity vector as illustrated in Fig. 1.

2) The fuel sample is spherical or cylindrical in the stagnation region.

3) The gas is ideal, with constant Pr, C_p, M, and $\rho\mu$; also, $Le=1$.

4) The gas-phase reaction is a second-order, one-step reaction: $F+N_0O_2\rightarrow P$.

5) The pyrolysis of the solid fuel follows an Arrhenius law.

6) Gas-phase radiation is negligible.

7) The temperature profile in the solid is one-dimensional and exponential.

Only those features of this model that differ from the standard stagnation-point diffusion flame formulation will be presented here. The momentum equation in the x direction is:

$$\rho u\frac{\partial u}{\partial x}+\rho v\frac{\partial u}{\partial y}-\frac{\partial}{\partial y}\left(\mu\frac{\partial u}{\partial y}\right)=\rho_e u_e\frac{\mathrm{d}u_e}{\mathrm{d}x}\left[1+\frac{\rho-\rho_e}{\rho_e}\frac{g_x}{u_e(\mathrm{d}u_e/\mathrm{d}x)}\right] \tag{1}$$

A density characteristic of the boundary-layer flame is defined as ρ^*. This characteristic density is used in the definition of a densimetric Froude number:

$$\phi=\frac{\rho^*-\rho_e}{\rho_e}\frac{g_x}{u_e(\mathrm{d}u_e/\mathrm{d}x)} \tag{2}$$

Received May 27, 1986; revision received Oct. 31, 1986.

*Graduate Student, Department of Mechanical and Aerospace Engineering; currently at Boeing Aircraft Company.

†Professor, Department of Mechanical and Aerospace Engineering. Associate Fellow AIAA.

At the stagnation point,

$$gx = (-gx)/R \tag{3}$$

$$u_e = a_f x \tag{4}$$

where a_f is the forced-flow velocity gradient. For a cylinder, $a_f = 2U_\infty/R$ and for a sphere, $a_f = 3/2U_\infty/R$. Since g_x and u_e have the same dependence on x, the forced- and natural-convection terms can be combined in a mixed-convection stretch rate:

$$a = a_f(1+\phi)^{1/2} \tag{5}$$

Substituting Eqs. (2-5) into Eq. (1) yields

$$\rho u\frac{\partial u}{\partial x} + \rho v\frac{\partial u}{\partial y} - \frac{\partial}{\partial y}\left(\mu\frac{\partial u}{\partial y}\right) = \rho_e a^2 x\left[1 + \left(\frac{\rho-\rho_e}{\rho^*-\rho_e}\right)\phi\Big/(1+\phi)\right] \tag{6}$$

with boundary conditions:

$$y=0: \quad u=0, \quad v=v_w$$

$$y\to\infty: \quad u = a_f x = ax/(1+\phi)^{1/2}$$

The variables a and ϕ characterize the mixed-convection boundary layer. For forced flow, $\phi=0$ and $a=a_f$. For natural convection, $\phi\to\infty$, $a_f=0$, and

$$a = \left[\left(\frac{\rho_e-\rho^*}{\rho_e}\right)\frac{g}{R}\right]^{1/2} \tag{7}$$

So the mixed-convection stretch rate a characterizes forced, mixed, and free convection.

Including an appropriate ρ^* in the definition of the Froude number makes the quantity

$$\left[1 + \left(\frac{\rho-\rho_e}{\rho^*-\rho_e}\right)\phi\right]\Big/(1+\phi)$$

in Eq. (6) approximately 1. If it were 1, the momentum equations would be independent of ϕ. Because ρ varies through the boundary layer, this quantity will always have some effect on the momentum equation. Also, because ϕ appears in the boundary conditions, it can never be eliminated from the formulation. By using ρ^*, the dependence of the momentum equation on ϕ is reduced but not eliminated.

The second feature of this model that differs from the standard stagnation-point diffusion flame formulation is the inclusion of surface radiation. This effect appears in the energy balance at the wall:

$$k_w\left(\frac{\partial T}{\partial y}\right)\Big|_{y\to 0^+} = \rho_w v_w(C_p T_w - C_s T_0 + L^*) + \epsilon\sigma T_w^4 \tag{8}$$

This equation is derived assuming that the heat transfer in the solid is one-dimensional. Therefore, the solid temperature profile is an exponential decay from T_w at $y=0$ to T_0 at $y\to-\infty$. Also, it has been assumed that $T_w^4 \gg T_e^4$.

The momentum, energy, and species equations can be nondimensionalized by a Dorodnitsyn-Howarth transform. A stream function is defined:

$$\psi(\xi,\eta) = \sqrt{\xi} f(\eta)$$

At the mixed-convection stagnation point,

$$\eta = \frac{ax^{(i+1)}}{2\sqrt{\xi}}\int_0^y \rho\,dy \qquad \xi = \int_0^x \rho_e\mu_e a x^{(2i+1)}dx$$

where $i=0$ is for the two-dimensional case (the fuel sample is cylindrical in the stagnation region) and $i=1$ is for the axisymmetric case (the fuel sample is spherical in the stagnation region). All calculations were done for $i=1$.

With $\theta = T/T_e$ and assuming $\rho\mu = \text{const}$, the transformed equations are

$$f''' + ff'' = \frac{1}{1+i}\left\{(f')^2 - 4\left[\theta + \left(\frac{\theta-1}{\theta^*-1}\right)\theta^*\phi\right]\Big/(1+\phi)\right\}$$

$$\frac{1}{Pr}\theta'' + f\theta' = -qw, \quad \frac{1}{Sc}Y_F'' + fY_F' = w$$

$$\frac{1}{Sc}Y_0'' + fY_0' = N_0 w, \quad w = DY_F Y_0 e^{-E/\theta} \tag{9}$$

where $D = B^*/a$ is the Damkohler number.

The boundary conditions are, at $\eta\to\infty$

$$f' = \frac{2}{(1+\phi)^{1/2}}, \quad \theta=1, \quad Y_0 = Y_{0e}, \quad Y_F = 0 \tag{10}$$

and at $\eta=0$

$$f_w' = 0, \quad f_w = -B_s e^{-E_s/\theta_w}$$

$$\theta_w' = -Prf_w\left[\theta_w + L - \frac{C_s}{C_p}\theta_0\right] + S\theta_w^4$$

$$Y_{F_w}' = Scf_w(1 - Y_{F_w}), \quad Y_{0_w}' = -Scf_w Y_{0_w} \tag{11}$$

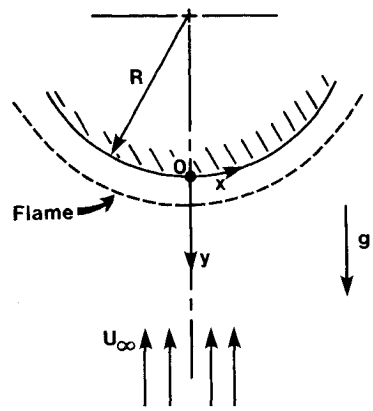

Fig. 1 Diffusion flame in the mixed-convection stagnation point of a solid fuel.

Table 1 Property values

Gas phase	
ρ_e	1.176 kg/m^3
ρ^*	0.261 kg/m^3
μ_e	1.85×10^{-5} kg/m-s
C_p	1.254 kJ/kg-K
T_e	300 K
T_{AF}	2400 K
k_e	2.93×10^{-5} kJ/m s-K
B^*	5.047×10^{7} 1/s
E^*	113 kJ/k-mole
q^*	25957 kJ/kg
Solid phase	
ρ_s	1180 kg/m^3
C_s	1.463 kJ/kg-K
T_0	300 K
B_s^*	2.32×10^{6} kg/m^2-s
E_s^*	125.6 kJ/k-mole
L^*	1050 kJ/kg

where

$$S = 1\left(\frac{\mu_e}{\rho_e a}\right)^{1/2} \frac{\sigma\epsilon}{k_e} T_e^3 \tag{12}$$

Table 1 gives the values for the fuel and gas properties. The fuel properties are those for PMMA given in Ref. 4. Table 2 describes the dimensionless variables. The radiation parameter S is of particular interest. The importance of surface radiation can be seen from the dimensionless formulation. Since S varies as $1/\sqrt{a}$, as a becomes small, the radiation parameter becomes large.

The value of θ^* used for the calculation is the average of the value of the nondimensional adiabatic flame temperature in air and the freestream temperature. This appears to be a reasonable choice, and it is easy to calculate a priori.

The problem has now been transformed into a ninth-order system of ordinary differential equations with nine boundary conditions. This system is solved numerically by introducing a fictitious unsteady term and constructing an explicit finite-difference scheme to march in time. Appropriate initial conditions are chosen, and the scheme either converges to a steady-state flame solution or to an extinction solution.

Results and Discussion

Effect of Surface Radiation

As can be seen from Figs. 2–5, the basic trends are the same for all ϕ, so T'ien's conclusions for the forced-flow case[4] apply. These will be summarized here, ignoring, for the moment the differences between forced and natural convection.

Table 2 Dimensionless parameters

Parameter	Value	Parameter	Value
C_S/C_p	1.17	$\theta_0 = T_0/T_e$	1.0
$L = k^*/C_p T_e$	2.79	$D = B^*/a$	Variable
N_0	1.92		
$Pr = C_p\mu_e/k_e$	0.7	$S = \left(\frac{\mu_e}{\rho_e a}\right)^{1/2} \frac{\sigma\epsilon}{k_e} T_e^3$	Variable
$Sc = \mu_e/\rho_e D_e$	0.7		
$q = q^*/CpT_e$	69		
$E = E^*/RT_e$	45.3		
$E_S = E_S^*/RT_e$	50.3	$B_S = \left[\frac{2}{\rho_e\mu_e a(i+1)}\right]^{1/2} B_S^*$	Variable
$\theta^* = \frac{T_{AF}+T_e}{2T_e}$	4.5	ϵ	0 or 1
		i	1

There are two sets of curves in Figs. 2–5. One set is for the case without surface radiation ($\epsilon = 0$); the other is for the case with blackbody surface radiation ($\epsilon = 1$). Figure 2 shows how the dimensionless fuel burning rate $-f_w$ varies with flame stretch rate a. The dimensional fuel mass flux is proportional to $-\sqrt{a}f_w$. For the case without radiation, $-f_w$ decreases very slowly with increasing a until the blowoff limit is reached at $a = 90$ 1/s. The value of $-f_w$ has fallen by about 10% from its value at $a = 1.0$ 1/s. When radiation is included, $-f_w$ is everywhere lower than for the case without radiation and now $-f_w$ increases with a until the blowoff limit is reached at $a = 80$ 1/s. Even more striking is the existence of a second extinction limit. For a below 3 1/s, there are no steady-state flame solutions. The difference between the two cases is greatest at low a. These results can be explained in terms of the radiation parameter S [Eq. (12)].

This parameter represents another mechanism in addition to convection and conduction by which the flame loses heat. It appears in the energy balance at the fuel surface [Eq. (11)]. Any heat lost to radiation is not used to pyrolyze fuel, so $-f_w$ is lowered. The difference between the two cases is greatest at low stretch rate because $S \sim 1/\sqrt{a}$. Physically, the fuel mass flow is lower at low a. Even neglecting radiation, at low a the flame produces less heat, and so less fuel is pyrolyzed. The wall temperature, however, is relatively constant with a. Since the heat loss due to surface radiation depends only on the wall temperature, as a decreases, the fraction of heat lost to radiation increases. At

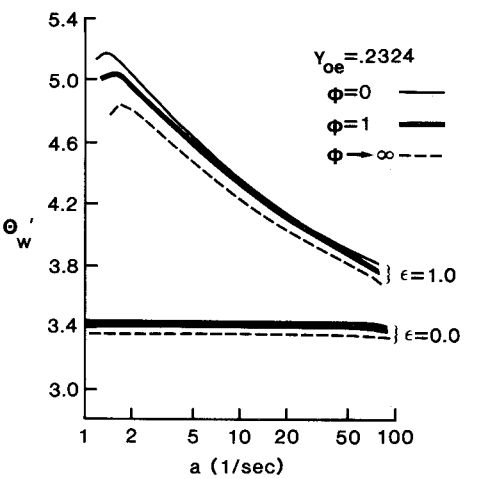

Fig. 3 Dimensionless wall heat-transfer rate vs mixed-convection stretch rate.

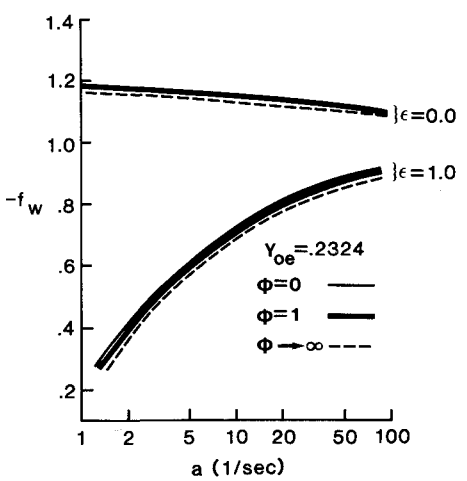

Fig. 2 Dimensionless fuel-burning rate vs mixed-convection stretch rate.

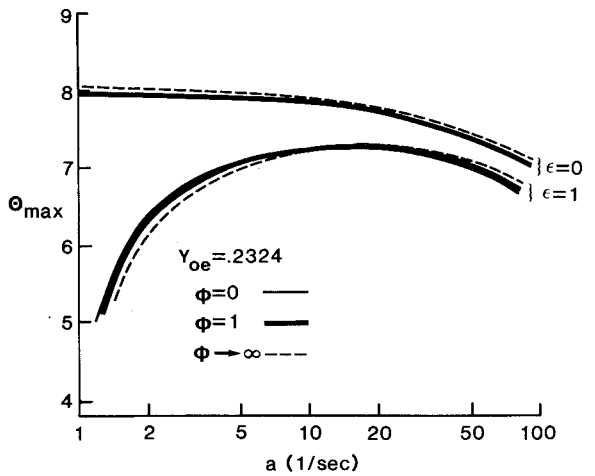

Fig. 4 Dimensionless maximum temperature vs mixed-convection stretch rate.

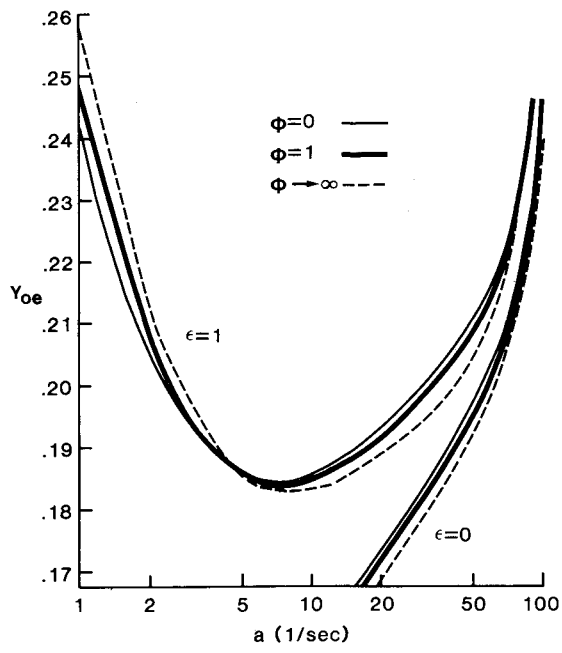

Fig. 5 Flammability boundary: limiting oxygen mass fraction vs mixed-convection stretch rate.

the lower limiting a, little heat goes to pyrolyzing fuel, and the flame extinguishes.

The dimensionless wall heat-transfer rate θ'_w is shown in Fig. 3. Dimensionally, the heat-transfer rate at the wall is proportional to θ'_w. Without radiation, θ'_w is constant with increasing a, showing only a slight decrease near the blowoff limit. With radiation included, θ'_w is higher. This means that a greater proportion of the heat generated by the flame is transferred to the wall. As a decreases, θ'_w increases, but $-f_w$ is not increasing. This implies that the increasing θ'_w is due to increased radiative surface heat loss, as a result of the $1/\sqrt{a}$ dependence of the radiation parameter S [see Eq. (11)]. Very near the radiative extinction limit, the curves dip slightly, indicating a very weak flame.

Figure 4 shows the variation of θ_{max} with a. Without radiation, the curves are fairly flat over a range of a; then θ_{max} decreases as the blowoff limit is approached. When the radiation term is included, θ_{max} is lowered, and the behavior at low a changes. Now θ_{max} falls dramatically as a is lowered. The increase in θ'_w described earlier has cooled the flame. Also, it can be seen that θ_{max} at the blowoff extinction limit is higher than θ_{max} at the radiative limit.

The existence of the radiative extinction limit can be seen clearly in Fig. 5, which shows how the limiting oxygen mass fraction varies with a. The curves in Fig. 5 are the extinction boundaries. A flame can exist for conditions above the line, and a flame cannot exist for conditions below the line. Without radiation the familiar blowoff extinction limit appears. There seems to be no fundamental oxygen limit. That is, no matter how low Y_{0e} is, there is a low enough stretch rate to allow a flame to exist. The situation is quite different for the case with radiation. Now there are two branches to the extinction boundary, which merge at a point that defines a fundamental limiting Y_{0e}. The high-speed branch is the blowoff limit. The low-speed branch is the radiative extinction limit. As Y_{0e} increases, the range of stretch rates that can support a flame broadens.

There is at least one piece of sketchy experimental evidence for the existence of this radiative limit. Ohtani et al.[10] investigated the bottom burning of PMMA samples of different sizes. In this configuration, the flame was in a natural-convection, stagnation-point boundary layer. One conclusion drawn was that there is a limiting sample size. For a sample larger than this size, no self-sustaining flame could exist. Referring to Eq. (7), this size limit corresponds to a minimum stretch rate that can support the flame. The same behavior is found in this numerical study when radiation is included in the model.

Comparison of Forced and Natural Convection

Although the results for different Froude numbers are similar, there are slight differences. Because the curve for $\phi=1$ always lies between the curves for $\phi=0$ and $\phi\to\infty$, the forced- and natural-convection curves represent two boundaries. Even when the curves cross, as they do in Figs. 4 and 5, all three curves cross at the same point. The following discussion will focus only on the extremes of forced and natural convection. A mixed-convection case would fall between these extremes.

There are two differences in the governing equations and boundary conditions for forced and natural convection. In the momentum equation (9), the last term differs by a factor of $[(1-1/\theta)/(1-1/\theta^*)]$ between the natural-convection case ($\phi\to\infty$) and the forced-convection case ($\phi=0$). Including θ^* in the definition of ϕ is an attempt to minimize the effect of this term, which as discussed, cannot be eliminated entirely. Some numerical experimentation was done with the different values of θ^*. Most of the variation in the curves could be eliminated by choosing $\theta^*=2.5$. Since no clear physical meaning could be found for choosing this θ^* over any other, the simple average of $\theta^*=(\theta_{AF}+1)/2$ was used here.

Changing θ^* changes the way a is defined. There are differences in the results that do not depend on a. These must be due to the different boundary conditions on the velocity at the edge of the boundary-layer Eq. (10). For forced convection, $f'(\infty)=2$; for natural convection, $f'(\infty)=0$. In Fig. 5, the minimum point on the limiting Y_{0e} curve is at a lower value of Y_{0e} for the natural-convection case than for the forced-convection case. No matter how a is defined, the value of Y_{0e} at the minimum point will not change. So, the natural-convection flame has a lower fundamental oxygen limit than the forced-convection flame.

This difference can be explained, at least in part, by Fig. 4. The value of θ_{max} at both extinction limits is higher for the natural-convection flames than for the forced-convection flames. Because near-limit natural-convection flames are slightly hotter than near-limit forced-convection flames, they can exist at a slightly lower Y_{0e}. Since this difference is due to the different boundary conditions on f', it is a result of the different velocity profiles at large η. There is a lower velocity for the natural-convection flame, so less heat is convected away, resulting in a hotter flame. These differences are very small. The value of θ_{max} at extinction is only 6% higher for the natural-convection flame. In the present calculation, the fundamental limiting Y_{0e} is 0.183 for the natural-convection flame and 0.184 for the forced-convection flame.

Conclusions

The extinction limits of a flame in the stagnation region of a solid fuel are investigated. The mixed-convection flow around the fuel sample is characterized by a Froude number and a mixed-convection stretch rate. The Froude number includes a characteristic density difference:

$$\phi=\left(\frac{\rho_e-\rho^*}{\rho_e}\right)\frac{g/R}{a_f^2}$$

It was found that this densimetric Froude number and the mixed-convection stretch rate can collapse the curves for different Froude numbers into a narrow band. As a result, most of the variation in flame behavior with Froude number is contained in the generalized stretch rate:

$$a=a_f(1+\phi)^{1/2}$$

One drawback to using the densimetric Froude number is that the characteristic density ρ^* depends on the flame's environment, so the advantages of using the densimetric Froude number are seen only for a range of conditions.

The extinction branch identified by T'ien[4] at small stretch rate also exists for the mixed- and natural-convection cases. This extinction branch is due to surface radiative loss. Even with rather high surface temperatures, radiative extinction occurs at very low stretch rate, so for most fuels and fuel geometries, it is likely to be observed only in reduced gravity. One important result is that there is a large difference between zero stretch rate and low stretch rate. While a steady flame may not be possible in a quiescent atmosphere, a low-speed forced flow or a low gravity level can provide an environment that can sustain a flame. Since low-speed air ventilation and small accelerations are present on a spacecraft, these types of flows must be considered for spacecraft fire-safety studies.

Acknowledgments

The first author acknowledges the support of a NASA Graduate Researcher Fellowship. The second author thanks NSF for support from NSF of MEA-8115339.

References

[1]Kumagi, S. and Isoda, H., "Combustion of Free Fuel Droplets in a Freely Falling Chamber," Thirteenth Symposium (International) on Combustion, The Combustion Institute, Pittsburgh, PA, 1970, pp. 779–785.

[2]Hall, A. L., "Observations of the Burning of a Candle at Zero Gravity," Naval School of Aviation Medicine, Rept. 5, Feb. 25, 1964; available from DDC as AD-436897.

[3]Cochran, T. H. and Masica, W. J., "Effects of Gravity on Laminar Gas Jet Diffusion Flames," NASA TN D-5872, 1970.

[4]T'ien, J. S., "Diffusion Flame Extinction at Small Stretch Rate: The Mechanism of Radiative Loss," *Combustion and Flame*, Vol. 65, 1986, pp. 31–34.

[5]Bonne, U., "Radiative Extinguishment of Flames at Zero Gravity," *Combustion and Flame*, Vol. 16, 1971, pp. 147–158.

[6]Sibulkin, M., Kulkarni, A. K., and Annamalai, K., "Effects of Radiation on the Burning of Vertical Fuel Surfaces," Eighteenth Symposium (International) on Combustion, The Combustion Institute, Pittsburgh, PA, 1981, pp. 611–617.

[7]Tsuji, H., "Counterflow Diffusion Flames," *Progress in Energy and Combustion Science*, Vol. 8, 1982, pp. 93–119.

[8]Fernandez-Pello, A. C. and Law, C. K., "On the Mixed-Convection Flame Structure in the Stagnation Point of a Fuel Particle," Nineteenth Symposium (International) on Combustion, The Combustion Institute, Pittsburgh, PA, 1982, pp. 1037–1044.

[9]T'ien, J. S., Singhal, S. N., Harrold, D. P., and Prahl, J. M., "Combustion and Extinction in the Stagnation-Point Boundary Layer of a Condensed Fuel," *Combustion and Flame*, Vol. 33, 1978, pp. 55–68.

[10]Ohtani, H., Hirano, T., and Akita, K., "Experimental Study of Bottom Surface Combustion of Polymethylmethacrylate," Eighteenth Symposium (International) on Combustion, The Combustion Institute, Pittsburgh, PA, 1981, pp. 591–599.

[11]Saitoh, T., "An Investigation of the Diffusion Flame Around a Porous Cylinder Under Conditions of Natural Convection," *Combustion and Flame*, Vol. 36, 1979, pp. 233–244.